Viscoelastic and Dielectric Behavior of a Polyisoprene/ Poly(4-*tert*-butyl styrene) Miscible Blend

Hiroshi Watanabe* and Yumi Matsumiya

Institute for Chemical Research, Kyoto University, Uji, Kyoto 611-0011, Japan

Jun Takada, Hiroshi Sasaki, Yoshiaki Matsushima, and Akira Kuriyama

Analytical Research Department, TOAGOSEI Co., Ltd, 1-1, Funami-cho, Minato-ku, Nagoya 455-0027, Japan

Tadashi Inoue

Department of Macromolecular Science, Faculty of Science, Osaka University, Toyonaka, Osaka 560-0043, Japan

Kyung Hyun Ahn

School of Chemical and Biological Engineering Seoul National University, Seoul 151-744, South Korea

Wei Yu

Department of Polymer Science and Engineering, Shanghai Jiao Tong University, Shanghai 200240, P. R. China

Ramanan Krishnamoorti

Department of Chemical Engineering, University of Houston, Houston, Texas 77204-4004

Received March 22, 2007; Revised Manuscript Received May 30, 2007

ABSTRACT: Linear viscoelastic and dielectric measurements were conducted for a blend of polyisoprene (PI, $M = 19._9 \times 10^3$) and poly(4-*tert*-butyl styrene) (PtBS, $M = 69._5 \times 10^3$) with a PI/PtBS composition of 8/2 (w/w). In general, PI and PtBS exhibit the lower-critical-solution-temperature (LCST) type phase behavior. At temperatures examined, $T \leq 70$ °C, our PI/PtBS blend was in a statically homogeneous state. The PI chain has the so-called type-A dipoles parallel along the backbone, and its large-scale (global) motion activates prominent dielectric relaxation, while the PtBS chain has no type-A dipoles and its global motion is dielectrically inert. In fact, at angular frequencies ω between 10^1 s^{-1} and 10^5 s^{-1} and at $T \leq 70$ °C, the dielectric signal of the blend was exclusively attributed to the PI chains therein. The time−temperature superposition failed for the dielectric loss ϵ'' of the PI chains, despite the fact that the blend was statically homogeneous. This result suggested that the frictional environment for the global motion was not the same for all PI chains. Namely, the PtBS chains relaxed more slowly than PI (as revealed from comparison of G^* and ϵ'' data) and their dynamic concentration fluctuation was frozen in the time scale of PI relaxation to give a spatially nonuniform frictional environment for the PI chains. The magnitude of this frictional nonuniformity changed with T thereby leading to the failure of the time−temperature superposition for PI. In contrast, the superposition worked excellently for the viscoelastic modulus ΔG^* of the PtBS chains (obtained by subtracting the PI contribution from the blend modulus). This result suggested that the PI chains relaxing faster than PtBS erased the heterogeneity in the time scale of the PtBS relaxation to provide all PtBS chains with the same frictional environment thereby allowing this relaxation to obey the superposition.

1. Introduction

In general, chemically different polymer chains are immiscible because of a decrease of the mixing entropy with increasing molecular weight.[1] However, many pairs of polymers are known to be miscible in a fairly wide range of temperature and composition.[1−19] Binary blends of those polymers offer interesting subjects of research in the field of polymer dynamics: Even in the statically homogeneous blend, the concentration of the components cannot be completely uniform in the segmental length scale because the same chemical species (monomers) tend to be locally concentrated due to the chain connectivity.[6−9] In addition to this self-concentration effect, the segment of a given chain component may have an intrinsic friction determined by the motional barrier within the chain, and the segmental relaxation processes of the two components do not necessarily occur simultaneously.[6−9] Furthermore, the component concentration may fluctuate dynamically over various length scales.[6−9,17−19] This type of *dynamic heterogeneity* can broaden the relaxation of respective component chains, in particular the local segmental relaxation. (In literature, the term "dynamic heterogeneity" is often utilized exclusively for representing the heterogeneity that broadens the segmental relaxation. However, throughout this paper, we utilize this term in a more general sense to represent "a transient, spatial nonuniformity of concentration in any length scale that vanishes on averaging over a sufficiently long time.")

* To whom correspondence should be addressed.

10.1021/ma070696h CCC: $37.00
Published on Web 06/30/2007

Extensive studies[1,6−9,12−15,17−20] have been made to elucidate the effects of the self-concentration, intrinsic friction, and dynamic heterogeneity on the segmental dynamics. Two separate glass transitions, the broad mode distribution of the segmental relaxation, and the thermorheological complexity of this distribution often observed for the statically homogeneous blends are attributed to these effects.[6−9,12−15,17−20]

The effect of the dynamic heterogeneity has been studied also for the terminal relaxation that reflects the *global* motion of the components over their chain size.[7,13−15,21−23] In particular, miscible blends of *cis*-polyisoprene (PI) and poly(vinyl ethylene) (PVE) were often chosen as model systems because only PI has the type-A dipole[24−26] and thus the terminal dielectric relaxation of the blends is exclusively attributed to the global motion of PI. Alegria and co-workers[7] and Urakawa and co-workers[13−15] made dielectric studies for the PI/PVE blends to observe the thermorheological complexity of the segmental relaxation attributable to the self-concentration and dynamic heterogeneity. In particular, Urakawa and co-workers[13,15] utilized the dielectrically detected global relaxation time of PI as a time giving a reference length scale in the blend (=end-to-end distance of the PI chain) and demonstrated that the length scale for the segmental relaxation is different for PI and PVE as expected from the concept of self-concentration. However, they observed no change of the terminal relaxation mode distribution of PI even when the dynamic heterogeneity changed with T.[13,15] Haley and co-workers[21,22] and Pathak and co-workers[23] combined the concepts of double reptation and self-concentration to examine the relaxation of the PI/PVE blends. The terminal mode distribution was found to change with the blend composition. However, this result simply reflected the changes in the entanglement molecular weight and segmental friction on blending, and no change of the terminal mode distribution directly attributable to the dynamic heterogeneity was observed.

Despite these experimental results, we expect an interesting possibility of terminal mode broadening due to the dynamic heterogeneity *under some conditions*. If the intrinsic segmental friction is much larger for one component (e.g., component B) than for the other component (A) and component B relaxes much more slowly compared to component A, the dynamic concentration fluctuation over the length scale comparable to the size R_B of the B chains (occurring through their global motion) should be effectively frozen during the terminal relaxation of component A. Under this condition, the effective segmental friction would not be the same for all A chains if their size R_A is smaller than R_B: During the terminal relaxation of the A chains, they exhibit the global motion over a distance $\sim R_A < R_B$. Then, some A chains would remain in a transiently B-enriched region during this relaxation and feel a larger friction (due to the slow B chains) compared to the other A chains. This frictional nonuniformity possibly broadens the terminal modes of the ensemble of all A chains. This broadening effect would become detectable when the slow component B is fairly dilute and its concentration fluctuation amplitude is at an adequate level. (It would be obvious that all A chains cannot simultaneously interact with the B chains and cannot feel the same friction *if* the B chain concentration is well below its overlapping concentration, although an experiment in such an extreme condition is not easily conducted.)

In the blends of long PVE chains and relatively short PI chains, PVE and PI correspond to the slow and fast components B and A, respectively. The lack of the effect of the dynamic heterogeneity on the terminal mode distribution of PI in these blends, noted in the previous studies,[13,15,21−23] is probably related to the difference of the intrinsic segmental frictions of PI and PVE as well as the PVE concentration: The difference of the intrinsic frictions, reflected in a difference of the bulk glass transition temperatures, $T_{g,PI} \cong -70$ °C and $T_{g,PVE} \cong 0$ °C, appears to be too small to give a detectably large effect on the global dynamics of PI. Furthermore, the PVE concentration examined in the previous studies (much higher than the overlapping concentration of PVE) could have been too large to enhance this effect.

In relation to this point, we remember that poly(4-*tert* butyl styrene) (PtBS) and PI exhibit the lower-critical-solution-temperature (LCST) type phase behavior.[16] A surprisingly large miscibility window is available for the PI/PtBS blends, as reported by Yurekli and Krishnamoorti.[16] In addition, the intrinsic segmental frictions of PI and PtBS should be significantly different, as judged from a huge difference of their bulk T_g, $T_{g,PI} \cong -70$ °C and $T_{g,PtBS} \cong 150$ °C.[16] Furthermore, PtBS chains have no type-A dipole and its global motion is dielectrically inert, which enables us to separate the terminal relaxation processes of PI and PtBS in PI/PtBS blends by combining the dielectric and viscoelastic data. For these reasons, the PI/PtBS blend is expected to serve as a good model system for a test of the effect of dynamic heterogeneity on the global chain motion.

Thus, we have examined the linear viscoelastic and dielectric behavior of a PI/PtBS blend. The dielectric signal reflecting the global relaxation of PI did not obey the time−temperature superposition, as anticipated from the above argument for the dynamic heterogeneity. Furthermore, combination of the dielectric and viscoelastic data enabled us to examine the global relaxation of the PtBS chains. The time−temperature superposition worked excellently for the PtBS relaxation, possibly because the PI chains relaxed more quickly than the PtBS chains thereby erasing the heterogeneity in the time scale of the PtBS relaxation. This paper presents details of these results.

Table 1. Characteristics of Samples

code	$10^{-3}M_w$	M_w/M_n
PtBS-70	69.5	1.03
PI-20[a]	19.9	1.10
PS-40	39.7	1.05

[a] Supplied from Kuraray Co.

2. Experimental Section

2.1. Materials. Poly(4-*tert*-butyl styrene) (PtBS) and polystyrene (PS) samples, both being anionically synthesized in our laboratory, and a commercially available polyisoprene sample (PI; supplied from Kuraray Co.) were used. The PI sample was fully characterized in our previous study.[27] The PtBS and PS samples were characterized in this study with GPC (CO-8020 and DP8020, Tosoh) equipped with a refractive index (RI)/low-angle light scattering (LALS) monitor (LS-8000, Tosoh). Tetrahydrofuran (THF) was the eluent, and commercially available monodisperse polystyrenes (TSK's, Tosoh) were utilized as the elution standards as well as the reference material for the RI/LALS signal intensities. The weight-average molecular weight M_w was determined from the LALS measurement, and the polydispersity index (M_w/M_n) was evaluated from the LALS measurement and elution volume calibration. Table 1 summarizes the characteristics of the samples. The sample code numbers refer to $10^{-3}M_w$.

The material subjected to the viscoelastic and dielectric tests was a PI-20/PtBS-70 blend with the PI/PtBS composition of 8/2 (w/w). For comparison, bulk PI-20 and PtBS-70 samples as well as a PI-20/PS-40 blend with the PI/PS composition of 8/2 (w/w) were also examined.

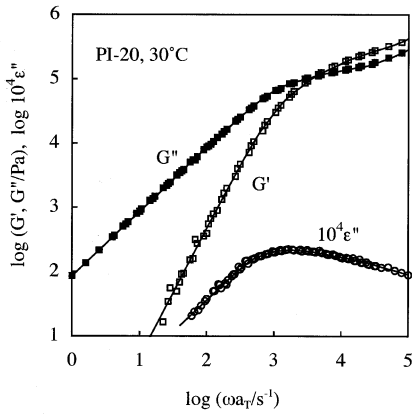

Figure 1. Storage and loss moduli, G' and G'', and dielectric loss, ϵ'', obtained for the bulk PI-20 sample. The ϵ'' data are multiplied by a factor of 10^4 and compared with the moduli data. The time−temperature superposition held excellently for those data, and the data reduced at 30 °C are shown.

The PI-20/PtBS-70 blend was prepared with the method reported by Yurekli and Krishnamoorti.[16] Prescribed weights of PI-20 and PtBS-70 (8/2 w/w) were dissolved in THF at the total concentration of 10 wt %, and this THF solution was drop-wisely poured in an excess methanol/acetone 8/2 mixture vigorously stirred with a magnetic bar. The precipitated blend was recovered *via* decantation and thoroughly dried in vacuum, first at room temperature and then at 85 °C. The PI-20/PtBS-70 blend thus prepared was transparent.

The PI-20/PS-40 blend with the PI/PS composition of 8/2 (w/w) was prepared with the same procedure. This blend was heavily turbid because the PI-20 and PS-40 chains having fairly large M were incompatible and fully phase-separated at around the room temperature. The PI-20 chains (major component) formed a continuous matrix phase in which the discrete, glassy domains (powders) of PS-40 were dispersed.

2.2. Measurements. The PI-20/PtBS-70 blend (8/2 w/w) was subjected to a small-angle X-ray scattering (SAXS) experiment at 25 and 70 °C. Dr. Matsuba and Prof. Kanaya at Kyoto University did us the great courtesy of making the experiment at Photon Factory, KEK (Tsukuba, Ibaraki 305-0801, Japan). The blend was confirmed to be statically homogeneous at $T \leq 70$ °C. This result was consistent with the negative interaction parameter χ between PI and PtBS reported in literature.[16]

Linear viscoelastic measurements were conducted for the PI-20/PtBS-70 blend at $T = 30$, 50, and 70 °C (in the statically homogeneous state) with a laboratory rheometer (ARES, Rheometrics). A homemade parallel-plate fixture was used. (This fixture was also utilized as the electrodes, as explained below.) The oscillatory strain amplitude was kept small (≤ 0.1) to ensure the linearity of the storage and loss moduli $G'(\omega)$ and $G''(\omega)$ measured as functions of the angular frequency ω in a range between 10^{-2} and 10^2 s^{-1}.

The homemade parallel-plate fixture was composed of the main and counter electrodes, with the former being surrounded by a guard electrode. The electrodes were made of stainless steel and electrically insulated with machinable ceramics and Teflon spacers. (This structure was very similar to that of a previously used rheo-dielectric cell.[28,29]) For the PI-20/PtBS-70 blend placed between the parallel-plate electrodes, dielectric measurements were conducted with the impedance analyzer (1260, Solartron) combined with the dielectric interface (1296, Solartron) in a range of ω between 10^1 and 10^5 s^{-1} at $T = 30$, 50, and 70 °C. No correction such as subtraction of a contribution from the direct current (dc) conductivity was made for the dielectric loss (ϵ'') data. (In fact, no dc conduction was detected in the range of ω and T examined.) Throughout this paper, the raw ϵ'' data are presented as the plots against the angular frequency ω, not the frequency f ($= \omega/2\pi$).

The bulk PI-20 and PtBS-70 samples as well as the PI-20/PS-40 blend were utilized as reference materials for the PI-20/PtBS-70 blend. The dielectric and viscoelastic measurements were made also for these materials.

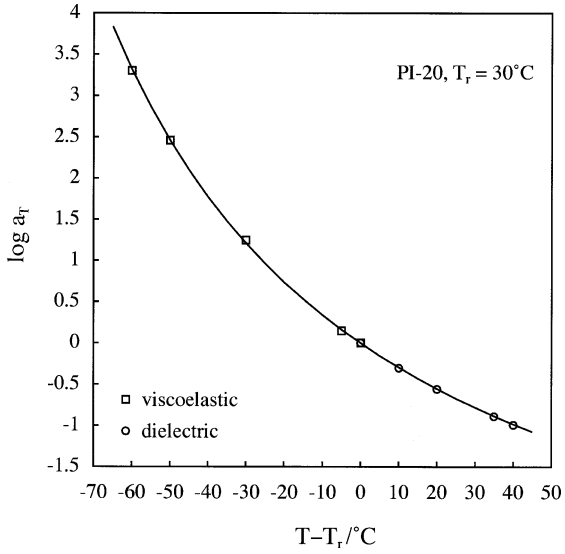

Figure 2. Shift factor a_T obtained for the viscoelastic G^* data (squares) and dielectric ϵ'' data (circles) of bulk PI-20 sample. The solid curve indicates the WLF eq 1.

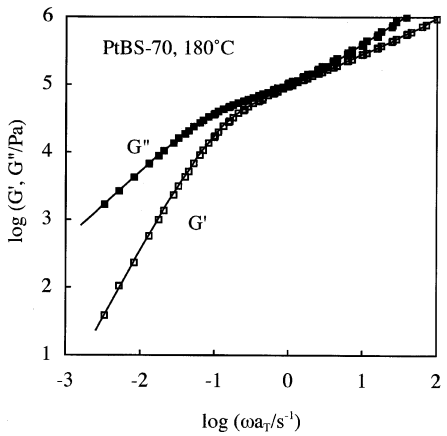

Figure 3. Storage and loss moduli, G' and G'', obtained for the bulk PtBS-70 sample. The time−temperature superposition held for these data, and the data reduced at 180 °C are shown. The PtBS chain having no type-A dipole exhibited no significant dielectric relaxation in the range of ω examined.

3. Results and Discussion

3.1. Dynamic Behavior of Bulk Components. Figure 1 shows the storage and loss moduli, $G'(\omega)$ and $G''(\omega)$, and the dielectric loss, $\epsilon''(\omega)$, measured for the bulk PI-20 sample. The ϵ'' data are multiplied by a factor of 10^4 and compared with the moduli data. The time−temperature superposition held excellently for the G^* and ϵ'' data (measured at T between −30 and +70 °C), and the data reduced at 30 °C are shown here. As noted from the ω dependence of the G^* data as well as the entanglement molecular weight for PI,[30,31] $M_e = \rho RT/G_N = 5.0 \times 10^3$ (ρ = density, R = gas constant, T = absolute temperature, and G_N = entanglement plateau modulus), the PI-20 chains having $M \cong 4M_e$ are moderately entangled in its bulk state. (The ϵ'' data of PI-20 agree, in both peak frequency and relaxation mode distribution, with literature data[24,25] accumulated for PI samples with small M_w/M_n values.)

Figure 2 shows the shift factor a_T obtained for the viscoelastic G^* and dielectric ϵ'' of PI-20. The a_T data for G^* and ϵ'' are

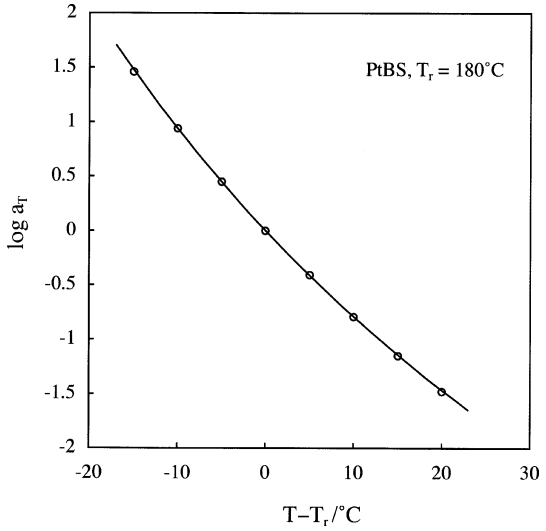

Figure 4. Shift factor a_T obtained for the G^* data of bulk PtBS-70 sample. The solid curve indicates the WLF eq 2.

indistinguishable and well described by a WLF equation shown with the solid curve,

$$\log a_T = -\frac{4.425(T - T_{r,bulk})}{140.0 + T - T_{r,bulk}} \text{ with } T_{r,bulk} = 30\ ^\circ\text{C} \quad \text{(for bulk PI)} \quad (1)$$

Equation 1 is equivalent to the previously reported WLF equation[32] (for which the reference temperature T_r was set at 40 °C).

The PI chain has the type-A dipole so that its global motion activates both of the terminal viscoelastic and dielectric relaxation processes having the same a_T; cf. Figures 1 and 2. This feature enables us to utilize the dielectric data of PI/PtBS blend to specify the viscoelastic modulus of PI therein, as explained later in more details.

Figure 3 shows the G' and G'' data of the bulk PtBS-70 sample. Since the PtBS chain has no type-A dipole, no dielectric relaxation was observed in the range of ω examined.[33] (The segmental relaxation of PtBS is dielectrically active but occurs at high ω not covered in our measurement.) The time−temperature superposition held for the G' and G'' data (measured at T between 165 and 200 °C), and the data reduced at 180 °C are shown here. In Figure 4, the shift factor a_T for this superposition is shown with the circles. The solid curve indicates a WLF equation determined for these a_T data,[34]

$$\log a_T = -\frac{10.0(T - T_{r,bulk})}{116.5 + T - T_{r,bulk}} \text{ with } T_{r,bulk} = 180\ ^\circ\text{C (for bulk PtBS)} \quad (2)$$

PtBS-70 sample exhibits neither a clear plateau of G' nor a peak of G''; cf. Figure 3. Thus, the PtBS-70 chains are barely entangled in their bulk state, as also expected from their M value ($= 69._5 \times 10^3 \cong 1.8M_e$ with $M_e = \rho RT/G_N = 37._6 \times 10^3$ for PtBS[35]). In fact, the viscoelastic mode distribution of bulk PtBS-70 is close to that for the Rouse chain, as shown later in Figure 10.

3.2. Structure in the Blend. SAXS measurements were conducted for the PI-20/PtBS-70 blend at 25 and 70 °C to examine the structure therein. The SAXS profile was azimuthally symmetric, and the circularly averaged SAXS intensity $I(q)$ (corrected for the background scattering) is plotted against the wave vector q in Figure 5. The solid curves indicate the intensity

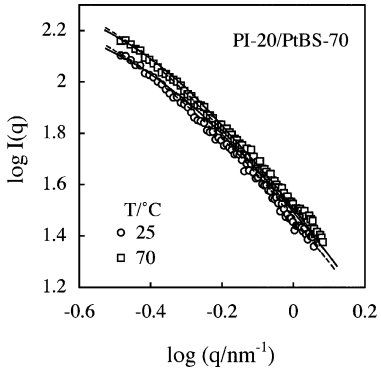

Figure 5. SAXS intensity $I(q)$ obtained for the PI-20/PtBS-70 blend with the PI/PtBS composition of 8/2 (w/w) at 25 and 70 °C. The circularly averaged intensity is plotted against the wave vector q. The solid curves show the intensities at 70 and 25 °C (upper and lower curves) calculated with the random phase approximation, and the dotted curves indicate the results of fitting with the Ornstein−Zernike equation. For further details, see text.

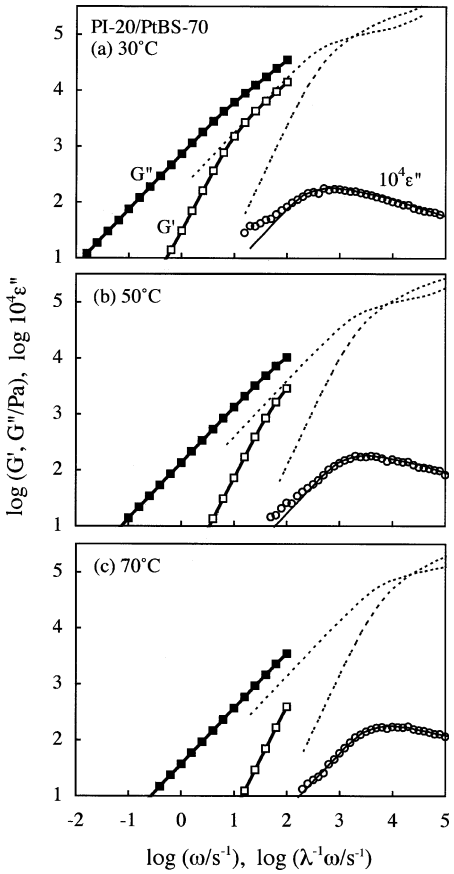

Figure 6. Storage and loss moduli, G' and G'', and dielectric loss, ϵ'', obtained for the PI-20/PtBS-70 blend with the PI/PtBS composition of 8/2 (w/w) at 30, 50, and 70 °C. The ϵ'' data (unfilled circles) are multiplied by a factor of 10^4 and compared with the G' and G'' data (unfilled and filled squares). These data are plotted against the angular frequency ω. Thin solid and dotted curves indicate the dielectric and viscoelastic data of bulk PI normalized by the PI volume fraction in the blend, $\phi_{PI}\epsilon''_{PI-bulk}(\omega)$ and $\phi_{PI}G^*_{PI-bulk}(\omega)$. These data are plotted against a reduced frequency ω/λ, with the shift factor λ being summarized in Figure 9. For further details, see text.

calculated with the random phase approximation (RPA). The plots show no hint of phase separation, confirming that the blend is statically homogeneous at $T \leq 70$ °C. This result is consistent with the negative interaction parameter χ between PI and PtBS reported by Yurekli and Krishnamoorti.[16]

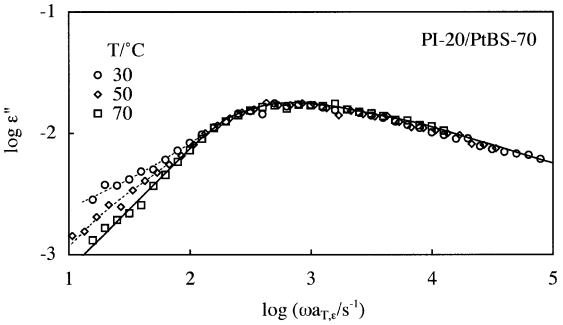

Figure 7. Test of the time−temperature superposability for the ϵ'' data of the PI-20/PtBS-70 blend with the PI/PtBS composition of 8/2 (w/w). The data at 50 and 70 °C are shifted along the ω axis by a factor of $a_{T,\epsilon}$ shown in Figure 9. The solid curve indicates the normalized dielectric data of bulk PI (identical to the thin solid curve shown in the top panel of Figure 6). The dotted curves are a guide for eye. For further details, see text.

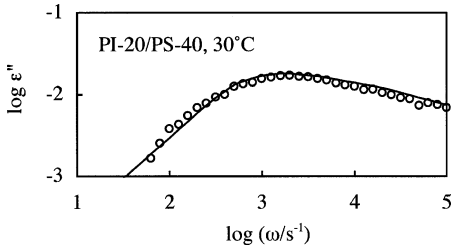

Figure 8. Dielectric loss data (circles) obtained for the PI-20/PS-40 blend with the PI/PS composition of 8/2 (w/w) at 30 °C. The solid curve indicates the normalized dielectric data of bulk PI at 30 °C, $\phi_{PI}\epsilon''_{PI-bulk}(\omega)$, being plotted against ω.

As a further test of this consistency, we compared the $I(q)$ data with the RPA scattering intensity given by[4,16,36,37]

$$I(q) = K\left\{\frac{1}{N_{PI}v_{PI}\phi_{PI}P_{PI}(q)} + \frac{1}{N_{PtBS}v_{PtBS}\phi_{PtBS}P_{PtBS}(q)} - \frac{2\chi}{v_0}\right\}^{-1} \quad (3a)$$

with

$$P_\xi(q) = \frac{2}{q^4 R_{g,\xi}{}^4}\{q^2 R_{g,\xi}{}^2 - 1 + \exp(-q^2 R_{g,\xi}{}^2)\}\ (\xi = \text{PI, PtBS}) \quad (3b)$$

Here, v_ξ, N_ξ, and ϕ_ξ represent the volume per repeating unit, the number of these units per chain, and the volume fraction of the component ξ (=PI, PtBS), respectively, v_0 is an arbitrarily chosen reference volume, and K is a constant determined by the scattering contrast of the two components. $P_\xi(q)$ is the Debye function for the component ξ determined by q and the unperturbed radius of gyration $R_{g,\xi}$. Utilizing empirical equations[35,38,39] excellently describing the R_g data of PI and PtBS in literature, we evaluated $R_{g,PI} = 4.7$ nm for PI-20 and $R_{g,PtBS} = 6.5$ nm for PtBS-70. Following Yurekli and Krishnamoorti,[16] we chose $v_\xi = v_0 = 100$ cm^3 mol^{-1} (ξ = PI, PtBS). The choice of $v_\xi = v_0$ does not introduce any uncertainty because the N_ξ value was calculated according to this choice.

For these values of R_g, v, and N, $I(q)$ was calculated from eq 3 with the χ parameter being chosen in the reported range,[16] $\chi = -0.014 \pm 0.004$ at 70 °C for $v_\xi = v_0 = 100$ cm^3 mol^{-1}. The front factor K was treated as a T-independent adjustable parameter. The $I(q)$ thus calculated for $\chi = -0.012$ was close to the $I(q)$ data at 70 °C, as shown with the upper solid curve in Figure 5. The $I(q)$ calculated for a smaller χ value of -0.017 (lower solid curve) was close to the $I(q)$ data at 25 °C. The

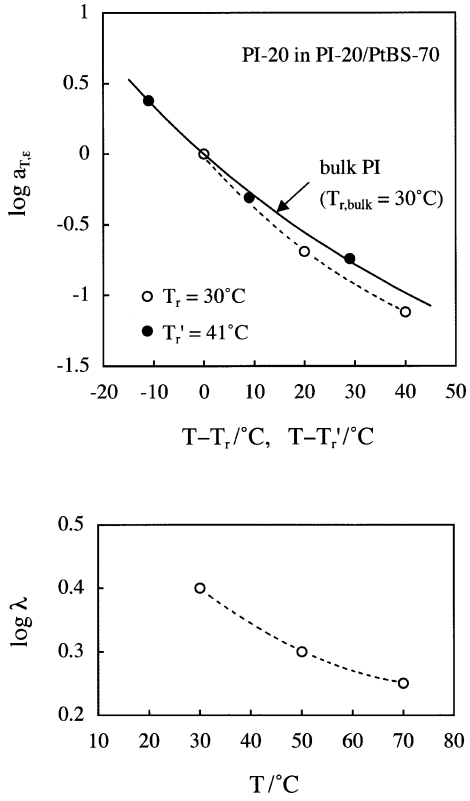

Figure 9. Top panel: Plots of the shift factor $a_{T,\epsilon}$ obtained in Figure 7 against a distance from the reference temperature T_r, $T - T_r$ with $T_r = 30$ °C. The solid curve indicates a_T of bulk PI plotted against $T - T_{r,bulk}$ with $T_{r,bulk} = 30$ °C (cf. eq 1). The filled circles denote a shift factor $a_{T,\epsilon}'$ for PI in the blend with respect to the iso-ξ reference temperature, $T_r' = 41$ °C. This $a_{T,\epsilon}'$ is plotted against $T - T_r'$. Bottom panel: Plots of the shift factor $\lambda(T)$ obtained in Figure 6 against T. In both of the top and bottom panels, the dotted curves are a guide for eye.

static homogeneity of the PI-20/PtBS-70 blend with this LCST feature (decrease of negative χ with decreasing T) is consistent with that found by Yurekli and Krishnamoorti.[16] From their χ data,[16] the phase separation temperature of our PI-20/PtBS-70 blend was roughly estimated to be $T_c \cong 250$ °C.[40]

It is also informative to estimate the correlation length ξ_c in the PI-20/PtBS-70 blend. For this purpose, the $I(q)$ data were fitted with the standard Ornstein−Zernike (OZ) equation (that coincides with the RPA equation at small q[36]),

$$I(q) = \frac{I(0)}{1 + \xi_c{}^2 q^2} \quad (4)$$

In Figure 5, the dotted curves indicate the results of fitting with ξ_c/nm = 0.42 (at 25 °C) and 0.47 (at 70 °C). These ξ_c values are of the order of segmental size b_s of the PI and PtBS chains, indicating that our blend at $T \ll T_c$ is *statically* homogeneous in the length scale well above b_s and only the concentration fluctuation having the wavelength $\cong b_s$ is stabilized for an infinitely long time (at equilibrium). However, this result does not necessarily mean that the PI/PtBS blend is completely homogeneous in the *dynamic sense* (the fluctuation having a longer wavelength may survive in the finite time scale of the terminal relaxation of PI, although its amplitude may be fairly small), as noted from the dielectric data of the blend examined below.

3.3. Overview of Dynamic Behavior of Blend. Figure 6 shows the G', G'', and ϵ'' data of the PI-20/PtBS-70 blend measured at 30, 50, and 70 °C; see symbols. The ϵ'' data (circles)

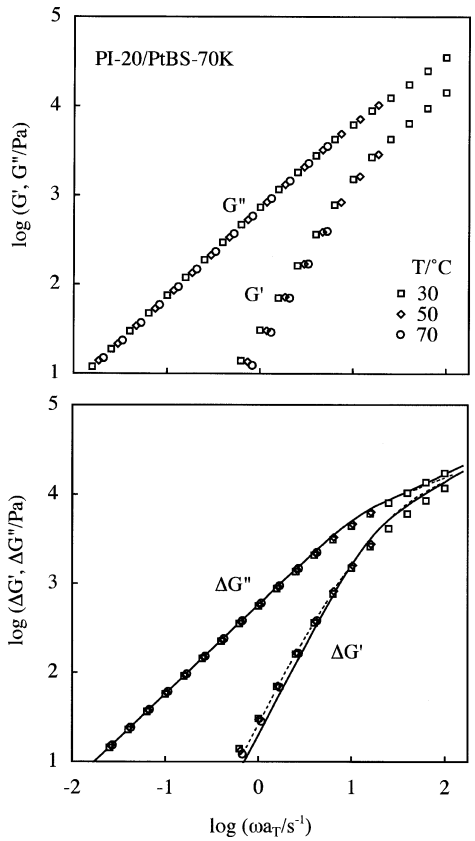

Figure 10. Test of the time−temperature superposability for the G_B* data of the PI-20/PtBS-70 blend (top panel) and the ΔG* data of the PtBS-70 chains in the blend (bottom panel). In the bottom panel, thin dotted curves indicate the normalized viscoelastic data of bulk PtBS, $\phi_{PtBS}G^*_{PtBS-bulk}(\omega)$, being plotted against a reduced frequency, ω/Λ with $\Lambda = 7.75 \times 10^{-3}$. The solid curve represents the modulus expected for the PtBS chains relaxing through the Rouse mechanism. For further details, see text.

are multiplied by a factor of 10^4 and compared with the G' and G'' data (unfilled and filled squares). Thin solid and dotted curves, respectively, indicate the dielectric loss and viscoelastic moduli of a majority of PI chains in the blend evaluated from the bulk PI data (Figure 1) with a method explained later.

The blend exhibits the linear viscoelastic flow behavior characterized with the terminal tails, $G' \propto \omega^2$ and $G'' \propto \omega$. From these tails, the terminal viscoelastic relaxation frequency of the blend, defined as a reciprocal of the second-moment average relaxation time (sometimes referred to as weight-average relaxation time),[26,31] is evaluated as

$$\omega_B = \left[\frac{\omega G''}{G'}\right]_{\omega\to 0} \cong 60\ s^{-1}\ (30\ °C),\ 380\ s^{-1}\ (50\ °C),\ \text{and}\ 1000\ s^{-1}\ (70\ °C) \quad (5)$$

Obviously, the terminal relaxation of the PI and PtBS component chains in the blend cannot be slower than that of the blend as a whole characterized by this ω_B.

For the PtBS chains having no type-A dipole, the segmental motion is dielectrically active. However, for those chains having the terminal relaxation frequency $\geq \omega_B \geq 60\ s^{-1}$, the segmental motion occurs at high ω ($>10^5\ s^{-1}$) not covered in our experimental window. Thus, the dielectric relaxation seen in Figure 6 is exclusively attributed to the global motion of the type-A PI chains. (The dielectrically active segmental motion of the PI chains occurs at high $\omega > 10^5\ s^{-1}$.)

Following this assignment, we compare the dielectric behavior of the PI chains in the blend with that in the bulk state. For this purpose, we normalized the $\epsilon''_{PI-bulk}$ data of bulk PI (Figure 1) by multiplying the PI volume fraction in the blend, $\phi_{PI} = 0.81$. In Figure 6, the thin solid curves indicate the normalized $\phi_{PI}\epsilon''_{PI-bulk}(\omega)$ data plotted against a reduced frequency ω/λ, where the $\lambda(T)$ is a factor that shifts the ϵ''-peak frequency ω_{peak} of bulk PI to ω_{peak} in the blend. These curves agree well with the ϵ'' data of the blend (circles) at ω around/higher than the ϵ''-peak frequency, indicating that the dielectric mode distribution is indistinguishable for the majority of the PI chains in the blend (giving the ϵ'' peak) and the chains in their bulk state. Consequently, the shift factor $\lambda(T)$ is equivalent to a ratio of the terminal relaxation times τ_ϵ of the majority of the PI chains in the blend and bulk at the same temperature:

$$\lambda(T) = \frac{\tau_\epsilon^{[blend]}(T)}{\tau_\epsilon^{[bulk]}(T)} \quad (6)$$

This $\lambda(T)$ factor is later discussed in relation to the dynamic heterogeneity in the blend.

Figure 6 also indicates that the normalized $\phi_{PI}\epsilon''_{PI-bulk}$ data at *low* ω do not agree with the ϵ'' data of the blend at 30 and 50 °C. This result suggests a failure of the time−temperature superposition for the PI chains in the blend. This failure is most clearly seen in Figure 7 where the ϵ'' data of the blend at 50 and 70 °C are shifted along the ω axis by an appropriate factor of $a_{T,\epsilon}$ to be best superposed on the data at a reference temperature, $T_r = 30$ °C.

As seen in Figure 7, the ϵ'' data of the blend at 50 and 70 °C excellently agree with the data at 30 °C at middle-to-high ω. Thus, the *majority* of PI chains (giving the ϵ'' peak) obeys the time−temperature superposition. However, at low ω, the ϵ'' data at 30 and 50 °C deviate upward from the data at 70 °C to violate this superposition. In addition, the terminal tail ($\epsilon'' \propto \omega$) is seen for the data at 50 and 70 °C but not at 30 °C in the range of ω examined. These results indicate that at 30 and 50 °C a small fraction of the PI chains relaxes more slowly than the majority. Furthermore, the agreement of the ϵ'' data of the blend at 70 °C with the normalized $\phi_{PI}\epsilon''_{PI-bulk}$ data of bulk PI (solid curve) suggests that the contribution of these slow PI chains to ϵ'' becomes undetectably small at 70 °C.

Here, a comment needs to be added for the lack of the terminal tail of the ϵ'' data at 30 °C. One may argue a possibility that this lack is attributed to the direct current (dc) conduction due to ionic impurities, not due to the relaxation of the slow, minor component of PI. However, for our PI-20/PtBS-70 blend at $\omega a_T > 10\ s^{-1}$, Figure 7 demonstrates that the terminal tail is observed at high T but vanishes at low T. This behavior is opposite to the usual dc conduction behavior, and the ϵ'' data of the blend at $T = 30$, 50, and 70 °C cannot be consistently described with the dc conduction mechanism, as explained in Appendix A. This result rules out the above possibility. Thus, the lack of the terminal tail of the blend at low T can be exclusively attributed to the slow, minor component of PI therein. The bulk PI system exhibits no hint of upturn of ϵ'' due to dc conduction in the range of $\omega a_T > 10\ s^{-1}$ at $T \leq 70$ °C (Figure 1), lending support to this assignment.

3.4. Effect of Dynamic Heterogeneity on PI Dynamics. As noted in Figure 6, the terminal viscoelastic relaxation of the blend is slower than the terminal dielectric relaxation, the latter exclusively attributed to the global motion of the majority of the PI chains: For example, at 70 °C, ϵ'' relaxes at $\omega_\epsilon \cong 10000\ s^{-1}$ (peak frequency) while G_B* relaxes at $\omega_B = 1000\ s^{-1}$ (eq 5). The relaxation of the blend as a whole is completed only after *both* of the components (PI and PtBS) exhibit the *global*

viscoelastic relaxation, and this relaxation of PI occurs simultaneously with the dielectric relaxation (as well-known from extensive data[24−26,28,29,32]). Thus, the difference between ω_ϵ and ω_B ($<\omega_\epsilon$) unequivocally indicates that the terminal relaxation is slower for the PtBS chains than for the PI chains. Then, during the PI relaxation, the dynamic heterogeneity due to the concentration fluctuation of PtBS is effectively *frozen* at a length scale L_f comparable to the PtBS chain size, $R_{g,PtBS}$. The chain size, corresponding to the length scale for the terminal relaxation, is smaller for PI-20 ($R_{g,PI} = 4.7$ nm) than for PtBS-70 ($R_{g,PtBS} = 6.5$ nm). Furthermore, the PtBS concentration in the blend, $C_{PtBS} = 0.19$ g cm^{-3} (calculated under an assumption of volume additivity of PtBS and PI), is only twice of the overlapping concentration, $C_{PtBS}^* = 0.10$ g cm^{-3} (calculated from $R_{g,PtBS}$), and the PtBS chains are not significantly overlapping among themselves in the blend. Namely, the conditions required for the dynamic heterogeneity to affect the global motion of PI explained earlier seem to be satisfied. Thus, in the time scale of the terminal relaxation of PI, the segmental relaxation of PtBS and PI should be completed but the segmental friction for PI due to PtBS *cannot* be the same for all PI chains because the fluctuation of the PtBS concentration still survives over the length scale $L_f \geq R_{g,PI}$. In this sense, the PtBS chains should behave as *immobile* frictional obstacles for the terminal relaxation of PI.

Thus, during the terminal relaxation, some PI chains interact with locally concentrated PtBS to feel a larger friction and exhibit slower relaxation compared to the remaining PI chains (majority) that interact with less concentrated PtBS. This nonuniformity of the segmental friction for PI naturally broadens the dielectric mode distribution of the blend, and a change in the magnitude of the frictional nonuniformity with T leads to a change in this mode distribution, i.e., the observed failure of the time−temperature superposition. Specifically, the dielectric mode distribution becomes narrower with increasing T; cf. Figure 7. The mechanism(s) of this narrowing is discussed below.

The PI chains should have a larger segmental friction ζ in the blend than in their bulk system because of the interaction with the PtBS chains. This antiplasticizing effect for PI, being consistent with results of the WLF analysis explained in the next section, can be represented as an increase of the Vogel temperature T_V, the (hypothetical) temperature where both of the time−temperature shift factor a_T and the segmental friction ζ diverge. The bulk PI has $T_{V,bulk} = -110$ °C (cf. eq 1), and the majority of the PI chains in the blend have $T_V = -99$ °C > $T_{V,bulk}$ as shown later from the WLF analysis. The minor, slow PI chains interacting with more concentrated PtBS should have an even higher T_V. The WLF-type acceleration of the relaxation in a given interval of T is stronger for chains having a higher T_V. Thus, this acceleration is stronger for the minor, slow PI chains than for the majority (fast PI chains), meaning that the difference of the relaxation frequencies of the slow and fast PI chains is reduced and the dielectric mode distribution becomes narrower with increasing T.

The above discussion does not incorporate a change in the mixing state with T. In reality, the PI and PtBS chains exhibit the LCST phase behavior[16] and the PtBS chains would tend to be locally concentrated (in the time scale of PI relaxation) at high T. In an extreme case where the static segregation occurs (not at $T \leq 70$ °C), the PI chains are no longer mixed with the PtBS chains. This extreme case is mimicked in the *incompatible* polyisoprene/polystyrene blend (PI-20/PS-40 blend). Figure 8 shows the ϵ'' data at 30 °C (circles) measured for this blend. The data, exclusively attributed to the PI chains in the blend, agree with the normalized $\phi_{PI}\epsilon''_{PI-bulk}$ data of bulk PI at the same temperature without any shift of the ϵ''-peak frequency (solid curve). This agreement is naturally expected because the PI chains in the blend do not interact with the PS chains in the segregated domains and the frictional/thermodynamic environment in the PI matrix phase is identical to that in the bulk PI system.

Although the PI chains in the PI/PtBS blend are not statically segregated from the PtBS chains at temperatures examined for this blend ($\leq$70 °C), the enhancement of the local concentration of PtBS at high T could reduce the fraction of the slow PI chains and tend to narrow the dielectric mode distribution (as similar to the situation in the PI/PS blend).

The narrowing of the dielectric mode distribution of PI with increasing T is attributable to the above two factors, the reduction of the difference of the relaxation frequencies of the fast and slow PI chains and the decrease of the fraction of the slow PI chains. Since the phase separation temperature of our PI/PtBS blend estimated from the literature χ data[16] ($T_c \cong 250$ °C[40]) is much higher than the temperatures examined ($T \leq 70$ °C), the narrowing seen in Figures 6 and 7 seems to be mainly due to the first factor. However, the contribution from the second factor cannot be ruled out at this moment. Viscoelastic and dielectric tests for PI/PtBS blends having various compositions as well as various M_{PI} and M_{PtBS} would enable us to quantify this contribution. These tests are considered as an interesting subject of future work.

3.5. WLF Analysis for Majority of PI Chains. The shift factor $a_{T,\epsilon}$ obtained in Figure 7 reflects a change of the segmental friction for the majority of the PI chains in the blend with T. In the top panel of Figure 9, the $a_{T,\epsilon}$ data are plotted against a distance from the reference temperature, $T - T_r$ with $T_r = 30$ °C; see unfilled circles. For these data, we attempt to make a correction of the segmental friction ζ often made for concentrated homopolymer solutions.[30] In this correction, a reference temperature for the solution T_r' is chosen in a way that the fractional free volume f (that determines ζ) in the solution at T_r' coincides with f_r in a reference bulk system. Following this method and considering that the thermal expansion coefficient α_f of the fractional free volume is the same for PI in the blend and bulk, we changed the reference temperature for the blend from $T_r = 30$ °C to an iso-ζ (iso-f) temperature T_r' (determined to be 41 °C from WLF analysis[34]) and introduced a shift factor $a_{T,\epsilon}'$ with respect to this T_r'; $a_{T,\epsilon}' = a_{T,\epsilon} \times 10^{\Delta}$ with $\Delta = 4.425(T_r' - T_r)/(140.0 + T_r - T_r')$ being a logarithmic shift factor from iso-ζ T_r' to T_r evaluated with eq 1. (This correction procedure is essentially the same as that made by Chung and co-workers:[6] For the PI and PVE components in PI/PVE blends, they utilized the WLF coefficients C_1 and C_2 averaged for bulk PI and PVE to evaluate the segmental friction/relaxation time. Note that changes of C_1 and C_2 on a change of the reference temperature are determined by α_f.[30])

In the top panel of Figure 9, the filled circles indicate plots of $a_{T,\epsilon}'$ against $T - T_r'$ with $T_r' = 41$ °C. The plot agrees well with the solid curve representing the plot of a_T of bulk PI against $T - T_{r,bulk}$($T_{r,bulk} = 30$ °C; cf. eq 1), indicating that the thermal expansion coefficient α_f is indeed indistinguishable for PI in the blend and bulk. This agreement suggests that the majority of PI chains in the blend is anti-plasticized by PtBS and their Vogel temperature T_V is higher than $T_{V,bulk}$ (=−110 °C; cf. eq 1) by $\Delta T_V = T_r' - T_{r,bulk} = 11$ °C, i.e., $T_V = -99$ °C for PI in the blend. T_V should be even higher for the minor, slow component of the PI chains that broadens the low-ω tail of ϵ''

at low T. This difference of T_V for the slow and fast PI chains is responsible for the narrowing of the dielectric mode distribution with increasing T, as discussed in the previous section.

Now, we focus on the shift factor λ obtained in Figure 6. This factor is identical to a ratio of $\tau_\epsilon^{[blend]}(T)$ of the majority of PI in the blend to $\tau_\epsilon^{[bulk]}(T)$ in bulk at the *same* temperature, T; cf. eq 6. In the bottom panel of Figure 9, λ is plotted against T. We note that λ is larger than unity mainly because the PI chains in the blend have T_V higher than $T_{V,bulk}$. We also note that λ decreases with increasing T. This decrease also reflects the difference of the T_V and $T_{V,bulk}$. The WLF-type decrease of the relaxation time τ on an increase of T in a given interval is more significant for chains having a higher T_V, i.e., for the PI chains in the blend than those in bulk, which leads to the decrease of λ. In fact, we confirmed that a ratio of $\tau_\epsilon^{[blend]}(T')$ to $\tau_\epsilon^{[bulk]}(T)$ at two iso-ζ temperatures, $T' = T + \Delta T_V$ in the blend and T in bulk, is insensitive to T and close to unity.

3.6. Effect of Dynamic Heterogeneity on PtBS Dynamics. Differing from the dielectric data, the viscoelastic G_B* data of the blend are contributed from both of the PI and PtBS chains. It is highly desired to evaluate the viscoelastic modulus ΔG* of the PtBS chains by subtracting the PI contribution from the G_B* data. For this purpose, it is informative to compare the ϵ'' and G_B* data of the blend.

The terminal relaxation is slower for the PtBS chains than for the majority of PI chains, and the PtBS chains can be regarded as the immobilized obstacles for the PI relaxation in the sense explained earlier. Then, the viscoelastic relaxation intensity of those PI chains in the blend should be smaller than that of bulk PI by the factor of $\phi_{PI} = 0.81$ (as expected from extensive viscoelastic data for homopolymer blends[26,32,41]) and the relaxation time is longer in the blend by the factor of λ ($= \tau_\epsilon^{[blend]}(T)/\tau_\epsilon^{[bulk]}(T)$; cf. eq 6). In the blend at 30 and 50 °C, some PI chains relax more slowly compared to the majority to broaden the tail of ϵ'' as seen in Figures 6 and 7. However, the fraction of such slow PI chains is small and their contribution to the viscoelastic modulus can be safely neglected in our analysis. (Note that the terminal viscoelastic intensity of PI in the blend should scales as $\phi_{PI}^{2.3}$ *if* PtBS relaxes faster than PI, as expected from the dynamic tube dilation (DTD) mechanism[26,42] fully tested for PI/PI blends.[32,41] Similarly, the models by Haley and co-workers[21,22] and Pathak and co-workers[23] incorporating the double reptation mechanism (an approximate version of the DTD mechanism[42]) predict that this intensity scales as ϕ_{PI}^2 *if* PtBS relaxes faster than PI. However, in our blend, the PtBS chains relax more slowly than the PI chains. Such PtBS chains do not dilate the tube for the PI chains thereby giving the PI terminal intensity $\propto \phi_{PI}$.)

From the above consideration, we can utilize the modulus $G_{PI-bulk}$*$(\omega;T)$ of bulk PI (Figure 1) and the λ data (Figure 9) to evaluate the modulus $G_{PI-blend}$*$(\omega;T)$ of the PI chains in the blend as

$$G_{PI-blend}^*(\omega;T) = \phi_{PI} G_{PI-bulk}^*(\omega\lambda;T) \qquad (7)$$

In Figure 6, the thin dotted curves indicate plots of this $G_{PI-blend}$*$(\omega;T)$ against ω. Comparison of these curves and the G_B* data (squares) confirms that the terminal relaxation is considerably faster for PI than for the blend as a whole (and the PtBS chains therein).

Strictly speaking, the slowly moving PtBS chains in the blend could enlarge the entanglement lifetime for the PI chains therein to narrow the viscoelastic relaxation mode distribution of these PI chains, as suggested from extensive data for PI/PI and PS/PS blends.[26,32,41] However, this narrowing effect cannot be significant in our blend (and neglected in eq 7) because the PtBS chains are the minor component in the blend ($\phi_{PtBS} = 0.19$).

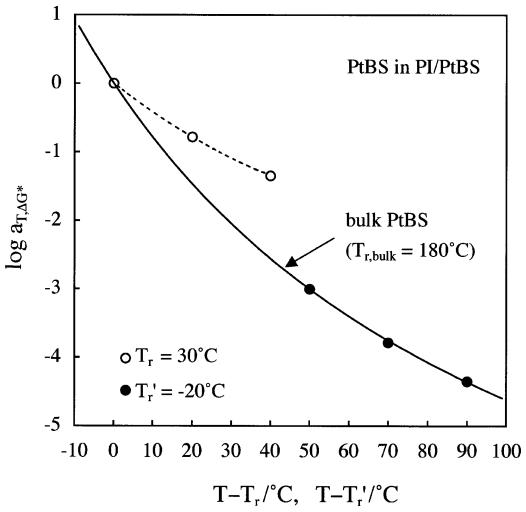

Figure 11. Shift factor $a_{T,\Delta G^*}$ (unfilled circles) for the PtBS-70 chains obtained in Figure 10. This factor is plotted against a distance from the reference temperature, $T - T_r$ with $T_r = 30$ °C. The solid curve indicates a_T of bulk PtBS plotted against $T - T_{r,bulk}$, with $T_{r,bulk} = 180$ °C (cf. eq 2). The filled circles denote a shift factor a_T' for PtBS in the blend with respect to the iso-ζ reference temperature, $T_r' = -20$ °C. This a_T' is plotted against $T - T_r'$. The dotted curve is a guide for eye.

Utilizing the $G_{PI-blend}$*$(\omega;T)$ thus obtained with eq 7, we evaluated the modulus of the PtBS chains in the blend as $\Delta G^*(\omega;T) = G_B^*(\omega;T) - G_{PI-blend}^*(\omega;T)$. In Figure 10, the time−temperature superposability is tested for the ΔG* data of PtBS (bottom panel) and for the G_B* data of the blend as a whole (top panel). The curves in the bottom panel indicate the normalized G* data of bulk PtBS and the Rouse modulus explained later.

In the top panel, the G_B'' data at 50 and 70 °C are shifted along the ω axis to superpose their low-ω tails ($G_B'' \propto \omega$) on the tail at 30 °C. The G_B' data are not well superposed with this shift, meaning that the blend as a whole does not obey the time−temperature superposition. This result reflects the difference of the shift factors a_T for the PI and PtBS chains in the blend.

In contrast, the same protocol of the shift gives excellent superposition of the storage and loss moduli of PtBS, $\Delta G'$ and $\Delta G''$; see the bottom panel. This result indicates that the dynamic heterogeneity possibly changes its magnitude with T but this change leads to no significant change of the distribution of the terminal relaxation modes of the PtBS chains (no change of the steady-state compliance of these chains). The PI chains, relaxing faster than the PtBS chains, should have erased the heterogeneity in the time sale of PtBS relaxation thereby allowing *all* PtBS chains to feel the same friction. For this case, the time−temperature superposition naturally holds for PtBS.

3.7. WLF Analysis for PtBS Chains. In Figure 11, the shift factor $a_{T,\Delta G^*}$ giving the excellent superposition of ΔG* (Figure 10) is plotted against the interval from the reference temperature, $T - T_r$ with $T_r = 30$ °C; see unfilled circles. The solid curve indicates plots of a_T of bulk PtBS against $T - T_{r,bulk}$ with $T_{r,bulk} = 180$ °C (cf. eq 2). The significant deviation of the $a_{T,\Delta G^*}$ data from this curve is indicative of strong plasticization for PtBS due to PI (=decrease of ζ of PtBS due to PI). We made the correction of segmental friction ζ for PtBS in the manner explained for Figure 9. The filled circles indicate plots of the

shift factor $a_{T,\Delta G^*}'$ with respect to the iso-ζ temperature, $T_r' = -20$ °C,[34] against $T - T_r'$; $a_{T,\Delta G^*}' = a_{T,\Delta G^*} \times 10^{\Delta}$ with $\Delta = 10.0(T_r' - T_r)/(116.5 + T_r - T_r')$ being a logarithmic shift factor from T_r' to T_r evaluated with eq 2. This $a_{T,\Delta G^*}'$ is indistinguishable from the a_T of bulk PtBS (solid curve), confirming that ζ of the PtBS chains in the blend at $T_r' = -20$ °C is the same as ζ of bulk PtBS chains at $T_{r,bulk} = 180$ °C. Correspondingly, ζ of PtBS in the blend at $T_r = 30$ °C coincides with ζ in the bulk at $T = T_{r,bulk} + T_r - T_r' = 230$ °C. This result is later utilized in our discussion of the relaxation mechanism of PtBS chains.

3.8. Relaxation Mechanism of PtBS in Blend. The relaxation mechanism of the PtBS chains in the blend can be examined for the ΔG^* data shown in the bottom panel of Figure 10. The solid curves represent the Rouse moduli[26,42]

$$G_{Rouse}^*(\omega) = \frac{\rho\phi_{PtBS}RT}{M_{PtBS}} \sum_{p\geq 1} \frac{i\omega\tau_{Rouse}/p^2}{1 + i\omega\tau_{Rouse}/p^2} \quad (i = \sqrt{-1}) \quad (8)$$

with ρ, ϕ_{PtBS}, and τ_{Rouse} being the blend density, PtBS volume fraction in the blend (=0.19), and the longest relaxation time (set at 0.052 s), respectively. The dotted curves indicate the G^* data of bulk PtBS at 180 °C (Figure 3) being multiplied by ϕ_{PtBS} and plotted against a reduced frequency, ω/Λ with $\Lambda = 7.75 \times 10^{-3}$. This Λ value corresponds to a change of the reference temperature for bulk PtBS from $T_{r,bulk} = 180$ °C to $T_r'' = 211$ °C; cf. eq 2.

The ΔG^* data coincide well with the $\phi_{PtBS}G^*$ data of bulk PtBS (dotted curves) as well as with G_{Rouse}^* (solid curves). This result, indicating no change of the Rouse-like distribution of the terminal relaxation modes of PtBS on blending, reflects the fact that the PtBS chains are barely entangled *among themselves* in the bulk as well as in the blend and the segmental friction is the same for all PtBS chains in the blend.

We should emphasize that this coincidence is expected even if the PtBS chains in the blend are entangled *with the PI chains*: For this case, the PtBS relaxation would be dominated by the constraint release (CR) mechanism[26,42] activated by the PI chains that relax considerably faster than the PtBS chains. The CR mechanism results in the Rouse-like relaxation, as revealed from extensive viscoelastic experiments for PS/PS and PI/PI blends.[26,32,41,43] Thus, the above coincidence itself does not allow us to distinguish the intrinsic (*entanglement free*) Rouse relaxation and CR−Rouse relaxation of the PtBS chains in the blend.

However, the WLF analysis of the shift factor (Figure 11) enables this distinction. The analysis suggested that the monomeric friction ζ of the PtBS chains in the blend at 30 °C coincides with ζ in the bulk at 230 °C, as explained earlier. Thus, the ΔG^* data at 30 °C should coincide with the $\phi_{PtBS}G^*$ data of bulk PtBS at 230 °C *if* the ΔG^* data reflect the intrinsic Rouse relaxation of PtBS in the blend. However, ΔG^* data actually coincide with the bulk PtBS data at 211 °C shown with the dotted curves in the bottom panel of Figure 10. This result indicates that the PtBS relaxation in the blend is slower than the intrinsic Rose relaxation by a factor of $10^{\Delta} = 7.8$, where Δ (=0.89) is a logarithmic shift factor for bulk PtBS from 230 °C to 211 °C evaluated with eq 2. This 10^{Δ} value is considerably larger than unity, suggesting that the PtBS relaxation in the blend is retarded by the entanglement with the PI chains. Thus, the Rouse-like relaxation of PtBS in the blend can be assigned as the CR relaxation activated by the motion of the PI chains. (This assignment in turn indicates that the PI chains are entangled with the more slowly relaxing PtBS chains, which is consistent with the analysis of the viscoelastic modulus of PI cast in the form of eq 7.)

4. Concluding Remarks

We have examined the linear viscoelastic and dielectric behavior of the PI-20/PtBS-70 blend with the PI/PtBS composition of 8/2 (w/w) in the statically homogeneous state at several temperatures, $T = 30$, 50, and 70 °C. The dielectric relaxation of the blend was exclusively attributed to the global motion of the PI chains therein. The PtBS chains relaxed more slowly than the PI chains.

The time−temperature superposition failed for the dielectric relaxation of PI. This result suggests that the dynamic heterogeneity due to the concentration fluctuation of PtBS was effectively frozen *in the time scale of the global relaxation of PI* and the PtBS chains behaved as heterogeneously distributed obstacles immobilized in this time scale at a length scale comparable to the PtBS chain size. These immobile obstacles give a nonuniform friction distribution for the PI chains: Some PI chains interacting with locally concentrated PtBS feel a larger friction and relax more slowly compared to the remaining PI chains (majority) that interact with less concentrated PtBS. A change in the magnitude of this frictional nonuniformity with T leads to a change in the dielectric mode distribution of the ensemble of all PI chains, which naturally results in the observed failure of the time−temperature superposition.

In contrast, the superposition worked excellently for the viscoelastic modulus of the PtBS chains (obtained by subtracting the PI contribution from the blend modulus). This result can be again related to the difference of the relaxation rates of the PI and PtBS chains (the former relaxing faster): In the time scale of the PtBS relaxation, the fast PI chains should have erased the dynamic heterogeneity to provide all PtBS chains with the same frictional environment. Then, the terminal relaxation mode distribution of the PtBS chains does not change with T and the time−temperature superposition holds accordingly.

Acknowledgment. We thank Dr. Matsuba and Prof. Kanaya at Kyoto University who did us the great courtesy of making the SAXS experiment. A suggestion from Prof. Lodge at University of Minnesota was very helpful for improving the discussion of the time−temperature superposability for the components in the blend. This work was partly supported by Heiwa-Nakajima Foundation and by Grant-in-Aid for Scientific Research on Priority Area "Soft Matter Physics" from the Ministry of Education, Culture, Sports, Science and Technology (Grant No. 18068009).

Appendix A. Test of the Dc Contribution to the Dielectric Data

The slow dielectric mode distribution of the PI-20/PtBS-70 blend broadens with decreasing T: see Figures 6 and 7. One may argue a possibility that this mode broadening is due to the direct current (dc) conduction that enlarges the dielectric loss ϵ'' at low ω, not due to the relaxation of the slow, minor component of PI. This possibility is examined below.

If the above argument is valid, the ϵ'' data of the blend at a temperature T are expressed as a sum of the PI contribution *with T-independent mode distribution*, $\epsilon_{PI}''(\omega;T)$, and the dc contribution, $\epsilon_{dc}''(\omega;T)$:

$$\epsilon''(\omega;T) = \epsilon_{PI}''(\omega;T) + \epsilon_{dc}''(\omega;T) \quad (A1)$$

The PI contribution, evaluated from the bulk PI data, has been shown with the thin solid curves in Figure 6. The dc contribution

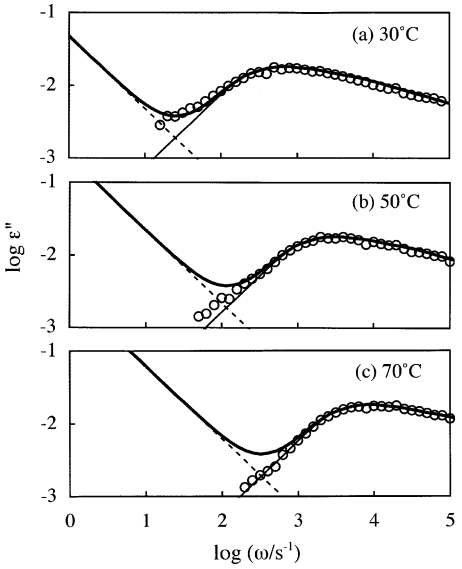

Figure 12. Test of the contribution of the dc conductivity to the ϵ'' data of the PI-20/PtBS-70 blend. The circles, thin solid curves, thin dotted curves, and thick solid curves, respectively, indicate the ϵ'' data, the PI contribution with T-independent mode distribution ϵ_{PI}'' (eq A3), the dc contribution ϵ_{dc}'' (eq A4), and the sum $\epsilon_{PI}'' + \epsilon_{dc}''$ expected for the case of dc-induced change of the mode distribution (eq A1). For further details, see Appendix A.

is generally expressed in terms of the dielectric permittivity of vacuum, ϵ_v, and the dc conductivity, σ, as[44]

$$\epsilon_{dc}''(\omega;T) = Q(T)/\omega \quad \text{with} \quad Q(T) = \sigma(T)/\epsilon_v \qquad \text{(A2)}$$

Here, we consider the temperature dependencies of $\epsilon_{PI}''(\omega;T)$ and $\epsilon_{dc}''(\omega;T)$. An increase of T leads to an acceleration of the PI relaxation as well as an enhancement of dc conduction, the latter usually reflecting an increase of the ionic mobility μ (and sometimes the enhancement of ionic dissociation). For the dielectric data of several polymers (including PI),[7,8,18,44,45] we observe that the dc conduction is enhanced with increasing T to a similar (or somewhat larger) extent as the acceleration of the segmental/global relaxation of the polymers; see, for example, Figure 8.18 of ref 44 and Figures 5 and 6 of ref 45. (In polymers having a specific interaction with the ions, the motion of the chain segment and ion appears to occur cooperaively[46−48] thereby giving similar T dependencies to $\epsilon_{polymer}''$ and ϵ_{dc}''.) For our PI/PtBS blend, the above observation allows us to relate the PI and dc contributions at two temperatures T_r and T ($>T_r$) as

$$\epsilon_{PI}''(\omega;T) = \epsilon_{PI}''(\theta_{PI}^{-1}\omega;T_r) \qquad \text{(A3)}$$

$$\epsilon_{dc}''(\omega;T) = \epsilon_{dc}''(\theta_{dc}^{-1}\omega;T_r), \quad Q(T) = \theta_{dc}Q(T_r) \qquad \text{(A4)}$$

with

$$\theta_{dc} \geq \theta_{PI} > 1 \qquad \text{(A5)}$$

Here, θ_{PI} denotes a ratio of the PI relaxation time τ at these temperatures, $\theta_{PI} = \tau(T_r)/\tau(T)$, and θ_{dc} is a ratio of the dc conductivity σ, $\theta_{dc} = \sigma(T)/\sigma(T_r)$. The θ_{PI} values are known from the ϵ''-peak frequency seen in Figure 6: $\theta_{PI} = 1$, 4.6, and 12.9 for T/°C = 30 ($=T_r$), 50, and 70 °C, respectively.

Now, we examine if the ϵ'' data of our PI/PtBS blend can be consistently described by eqs A1−A5. In Figure 12, the ϵ'' data, the PI contribution with T-independent mode distribution ϵ_{PI}'' (eq A3 with the above θ_{PI} values), the dc contribution ϵ_{dc}'' (eq A4), and the sum $\epsilon_{PI}'' + \epsilon_{dc}''$ expected for the case of dc-induced mode broadening (eq A1) are shown with the circles, thin solid curves, thin dotted curves, and thick solid curves, respectively. At 30 °C (Figure 12a), a choice of $Q_r = 0.048$ s^{-1} allows the sum to be fairly close to the ϵ'' data. If the argument of the dc-induced mode broadening is valid, the sum at 50 and 70 °C calculated with $Q = \theta_{dc}Q_r \geq \theta_{PI}Q_r$ should agree with the ϵ'' data at those T. Nevertheless, the minimum possible sum calculated for the minimum values of Q ($=\theta_{PI}Q_r$), shown with the thick solid curves in Figure 12, parts b and c, deviates upward from the data at low ω (circles). The deviation is enhanced for the sum calculated with the general value of $Q \geq \theta_{PI}Q_r$. This result unequivocally indicates that the argument of dc-induced mode broadening cannot describe the ϵ'' data consistently. Thus, the change of the mode distribution with T is attributed to the change of the relaxation frequency (and intensity) of the slow, minor component of PI.

Since PI has rather small type-A dipoles, this change of the mode distribution occurs at a considerably low level of ϵ'' ($<10^{-2}$; cf. Figure 12). It would be easier to detect the change if we could use a type-A polymer having larger dipoles as one component in the blend, although a choice of the other, non-type-A component may not be so easy. (The second component is required to be miscible with the first component in a wide range of T and its bulk T_g is to be much higher than that of the first component.)

References and Notes

(1) Utracki, L A. *Polymer Alloys and Blends*; Carl Hanser: Munich, Germany, 1989.
(2) Graessley, W. W.; Krishnamoorti, R.; Balsara, N. P.; Butera, R. J.; Fetter, L. J.; Lohse, D. J.; Schulz, D. N.; Sissano, J. A. *Macromolecules* **1994**, *27*, 3896.
(3) Reichart, G. C.; Graessley, W. W.; Register, R. A.; Krishnamoorti, R.; Lohse, D. J. *Macromolecules* **1997**, *30*, 3363.
(4) Sakurai, S.; Jinnai, H.; Hasegawa, H.; Hashimoto, T.; Han, C. C. *Macromolecules* **1991**, *24*, 4839.
(5) Schacht. P. A.; Koberstein, J. T. *Polymer* **2002**, *43*, 6527.
(6) Chang, G. C.; Kornfield, J. A.; Smith, S. D. *Macromolecules* **1994**, *27*, 964.
(7) Alegria, A.; Colmenero, J.; Ngai, K. L.; Roland, C. M. *Macromolecules* **1994**, *27*, 4486.
(8) Kumar, S. K,; Colby, R. H.; Anastasiadis, S. H.; Fytas, G. *J. Chem. Phys.* **1996**, *105*, 3777.
(9) Lodge, T. P.; McLeish, T. C. B. *Macromolecules* **2000**, *33*, 5278.
(10) Tambasco, M.; Lipson, J. E. G.; Higgins, J. S. *Macromolecules* **2006**, *39*, 4860.
(11) Takeno, H.; Koizumi, S. *Polymer* **2006**, *47*, 5946.
(12) Krygier, E.; Lin, G. X.; Mendes, J.; Mukandela, G.; Azar, D.; Jones, A. A.; Pathak, J. A.; Colby, R. H.; Kumar, S. K.; Floudas, G.; Krishnamoorti, R.; Faust, R. *Macromolecules* **2005**, *38*, 7721.
(13) Hirose, Y.; Urakawa, O.; Adachi, K. *Macromolecules* **2003**, *36*, 3699.
(14) Hirose, Y.; Urakawa, O.; Adachi, K. *J. Polym. Sci., Part B: Polym. Phys.* **2004**, *42*, 4084.
(15) Urakawa, O. *Nihon Reoroji Gakkaishi (J. Soc. Rheol. Japan*) **2004**, *32*, 265.
(16) Yurekli, K.; Krishnamoorti, R. *J. Polym. Sci., Part B: Polym. Phys.* **2004**, *42*, 3204.
(17) Wetton, R. E.; MacKnight, W. J.; Fried, J. R.; Karasz, F. E. *Macromolecules* **1978**, *11*, 158.
(18) Liang, K.; Banhegyi, G.; Karasz, F. R.; MacKnight, W. J. *J. Polym. Sci., Part B: Polym. Phys.* **1991**, *29*, 649.
(19) Miura, N.; MacKnight, W. J.; Matsuoka, S.; Karasz, F. E. *Polymer* **2001**, *42*, 6129.
(20) Zetsche, A.; Fischer, E. W. *Acta Polym.* **1994**, *45*, 168.
(21) Haley, J. C.; Lodge, T. P.; He, Y.; Ediger, M. D.; von Meerwall, E. D.; Mijovic, J. *Macromolecules* **2003**, *36*, 5142.
(22) Haley, J. C.; Lodge, T. P. *J. Rheol.* **2004**, *48*, 463.
(23) Pathak, J. A.; Kumar, S. K.; Colby, R. H. *Macromolecules* **2004**, *37*, 6994.
(24) Adachi, K.; Kotaka, T. *Prog. Polym. Sci.* **1993**, *18*, 585.
(25) Watanabe, H. *Macromol. Rapid Commun.* **2001**, *22*, 127.
(26) Watanabe, H. *Prog. Polym. Sci.* **1999**, *24*, 1253.
(27) Matsumiya, Y.; Inoue, T.; Watanabe, H.; Kihara, S.; Ohshima, M. *Nihon Reoroji Gakkaishi* (*J. Soc. Rheol. Japan*) **2007**, *35*, 155.

(28) Matsumiya, Y.; Watanabe, H.; Inoue, T.; Osaki, K.; Yao, M. L. *Macromolecules* **1998**, *31*, 7973.
(29) Watanabe, H.; Ishida, S.; Matsumiya, Y. *Macromolecules* **2002**, *35*, 8802.
(30) Ferry, J. D. *Viscoelastic Properties of Polymers*, 3rd ed.; Wiley: New York, 1980.
(31) Graessley, W. W. *Adv. Polym. Sci.* **1974**, *16*, 1.
(32) Watanabe, H.; Ishida, S.; Matsumiya, Y.; Inoue, T. *Macromolecules* **2004**, *37*, 1937.
(33) The bulk PtBS-70 sample exhibited just the direct current conduction at low ω in the dielectric measurements at temperatures examined in Figures 3 and 4 (=165−200 °C).
(34) The standard WLF analysis[30] is made by plotting the 1/log a_T data against $1/(T - T_r)$; $1/\log a_T = -1/C_1 - C_2/\{C_1(T - T_r)\}$ according to WLF equation. The WLF coefficients C_1 and C_2 appearing in eqs 1 and 2 were determined from the slope and intercept of this plot. The correction to an iso-ζ state (where the fractional free volume f has a given value f_{iso}) is made with the aid of the C_1 and C_2 values thus obtained. The f_r value at the reference temperature T_r and the thermal expansion coefficient of the fractional free volume α_f are determined as $f_r = 0.4343/C_1$ and $\alpha_f = 0.4343/C_1C_2$.[30] Then, the iso-ζ temperature T_r' (where $f = f_{iso}$) is determined as $T_r' = T_r + (f_{iso} - f_r)/\alpha_f$. The iso-$\zeta$ temperatures utilized in Figures 9 (top panel) and 11 were determined in this way.
(35) Fetters, L. J.; Lohse, D. J.; Colby, R. H. *Chain Dimension and Entanglement Spacing*; In Mark, J. E., Ed. *Physical Properties of Polymers Handbook* (2nd ed.), Springer: New York, 2007.
(36) de Gennes, P. G. *Scaling Concepts in Polymer Physics*, Cornell University Press: Ithaca, NY, 1979.
(37) Balsara, N. P.; Fetters, L. J.; Hadjichristidis, N.; Lohse, D. J.; Han, C. C.; Graessley, W. W.; Krishnamoorti, R. *Macromolecules* **1992**, *25*, 6137.
(38) Tsunashima, Y.; Hirata, M.; Nemoto, N.; Kurata, M. *Macromolecules* **1988**, *21*, 1107.
(39) Fetters, L. J.; Hadjichristidis, N.; Lindner, J. S.; Mays, J. W. *J. Chem. Phys. Ref. Data* **1994**, *23*, 619.
(40) Extrapolating the χ data[16] for PI ($M_{PI} = 40._0 \times 10^3$) and PtBS ($M_{PtBS} = 33._3 \times 10^3$) reported as a function of T, we estimated the phase separation temperature of the PI-20/PtBS-70 blend as $T_c \cong 250$ °C. Since these M values are not identical to those of PI-20 and PtBS-70, this T_c is to be regarded as a rough estimate.
(41) Watanabe, H.; Ishida, S.; Matsumiya, Y.; Inoue, T. *Macromolecules* **2004**, *37*, 6619.
(42) McLeish, T. C. B. *Adv. Phys.* **2002**, *51*, 1379.
(43) Sawada, T.; Qiao, X.; Watanabe, H. *Nihon Reoroji Gakkaishi* (*J. Soc. Rheol. Japan*) **2007**, *35*, 11.
(44) Kremer, F.; Schönhals, A. *Boardband Dielectric Spectroscopy*, Springer: Berlin, 2002.
(45) Ren, J.; Urakawa, O.; Adachi, K. *Macromolecules* **2003**, *36*, 210.
(46) Watanabe, M.; Ogata, N. *Br. Polym. J.* **1988**, *20*, 181.
(47) Gray, F. M. *Polymer Electrolytes: Fundamental and Technological Applications*; VCH Publishers: New York (1991).
(48) Kataoka, H.; Saito, Y.; Tabuchi, M.; Wada, Y.; Sakai, T. *Macromolecules* **2002**, *35*, 6239.

MA070696H